D. Vennerberg, M. R. Kessler: Anisotropic Buckypaper Through Shear-Induced Mechanical Alignment of Carbon Nanotubes in Water, Carbon, 2014, 80, 433-439. doi:10.1016/j.carbon.2014.08.082. © 2015, Elsevier.

Anisotropic buckypaper through shear-induced mechanical alignment of carbon nanotubes in water

Danny Vennerberg[a],
Michael R. Kessler[a, b]

[a] Dept. of Materials Science and Engineering, Iowa State University, Ames, IA, United States

[b] School of Mechanical and Materials Engineering, Washington State University, Pullman, WA, United States

Abstract

A simple method for aligning nanotubes in buckypaper with a modified Taylor–Couette system is reported. Using shear forces produced by a rotating cylinder to orient multi-walled carbon nanotubes in a surfactant-assisted aqueous dispersion, the suspended nanotubes are simultaneously aligned and filtered. The resulting buckypaper is composed of nanotubes with preferential orientation in the direction of flow and possesses anisotropic electrical and mechanical properties, which are both enhanced parallel to the direction of orientation. The technique presented here requires no specialized equipment and can be implemented with any type of carbon nanotube synthesized by any method. Furthermore, the size of the buckypaper sheets can be easily increased by adjusting the length and diameter of the cylinders in the setup, offering the possibility for low-cost production of large quantities of oriented buckypaper.

1. Introduction

Carbon nanotubes (CNTs) have been studied extensively over the last two decades because of their outstanding electrical, mechanical, and thermal properties, which makes them ideal candidates for use as reinforcement in multifunctional composites among other applications **[1]** and **[2]**. However, composites fabricated by mixing CNTs into a resin are limited to low loading levels because the large increases in viscosity that occur at higher loadings encumber processing. This, in turn, limits the effect that CNTs can have on the composite properties, and new methods must be developed if the true potential of CNT composites is to be realized. One way to achieve high loadings of CNTs in a resin is through the use of buckypaper (BP), which is

a free-standing mat of tightly packed CNTs formed by the controlled filtration of a CNT dispersion. BP can be handled in a manner similar to glass and carbon fiber mats, and traditional composite processing techniques such as compression molding and vacuum-assisted resin transfer molding can be used to infiltrate resin into the pores of the BP mat and bind several plies together into composites **[3]** and **[4]**. Using this approach, composites containing up to 60 wt.% MWCNTs have been achieved **[5]** and outstanding mechanical **[6]** and **[7]**, thermal **[8]**, electrical **[7]**, and electromagnetic shielding properties **[9]** have been realized in BP-reinforced polymers. Most BP is composed of CNTs that are randomly aligned. However, as with any fiber-reinforced composite, optimal properties are realized when the fiber alignment is unidirectional within each ply and the composite layup is judiciously tailored to match the expected stress state of its application.

Several methods to align CNTs within BP films have been reported recently, which can be broadly classified as alignment through (i) mechanical stretching of cross-linked CNT mats, (ii) pushing or pulling vertically-aligned carbon nanotubes (VACNTs), and (iii) the application of large magnetic fields. Mechanical stretching involves uniaxially straining randomly aligned multi-walled carbon nanotube (MWCNT) BP and then impregnating the stretched nanotube film with resin. Bismaleimide (BMI)/BP composites made with this process possessed outstanding mechanical and electrical properties **[5]** and, when the MWCNTs in the BP were functionalized with epoxide groups, the resulting composites exhibited unprecedentedly high strength (3081 MPa) and modulus (350 GPa), surpassing even high-performance carbon fiber composites **[10]**. However, the MWCNTs used in this study were cross-linked together through a specialized synthesis process necessary to prevent the BP from tearing at high strains, which excludes the method from widespread industrial use in the near future.

Highly aligned BP can also be produced from VACNT arrays, which consist of forests of densely-packed and highly aligned nanotubes. By pulling on a VACNT forest, van der Waals attraction among neighboring nanotubes causes the CNTs to assemble into continuous yarns or BP mats **[11]**, **[12]**, **[13]**, **[14]**, **[15]**, **[16]**, **[17]**, **[18]** and **[19]**. In addition to being spun by pulling action, VACNT forests can also be "pushed" down like dominos to form BP. This method has been implemented for vertically aligned MWCNTs using a cylinder to physically roll over and flatten the nanotube forest, and the BP produced in this manner exhibited higher electrical and thermal conductivity in the direction of alignment **[20]**. However, this method is also not amenable to large-scale use, as MWCNT forests with very high degrees of vertical alignment must be grown, a process that is currently only possible in a few laboratories.

Magnetic alignment is another nanotube orientation technique developed by Smalley **[21]** and refined by Liang and coworkers **[22]**. This method involves filtering CNTs in the presence of an applied magnetic field. Because CNTs have anisotropic magnetic susceptibilities, they tend to align with the direction of applied magnetic field lines in order to minimize energy. If a sufficiently strong magnetic field is applied to MWCNTs that are very well dispersed in solution, the MWCNTs will become oriented, and subsequent filtering will lead to the formation of aligned BP. Individual nanotubes comprising a MWCNT can be metallic or semiconducting depending on their structure with paramagnetic or diamagnetic responses to applied magnetic fields, respectively, both of which tend to align the MWCNT in the same direction and with nearly the same force **[23]**, **[24]** and **[25]**. However, huge magnetic fields on the order of 10–

30 T are required to produce observable degrees of alignment **[21]**. The cryogenically-cooled electromagnets needed to achieve those massive magnetic fields render this method unfit for the production of aligned BP on any appreciable scale.

An alternative approach for aligning nanotubes in BP is outlined in this paper. When subjected to shear forces in a fluid, CNTs align along the direction of flow. Using a modified Taylor–Couette system, an aqueous MWCNT dispersion is simultaneously sheared and filtered to produce BP with preferential nanotube orientation in the direction of flow. The aligned BP has anisotropic electrical and mechanical properties, which are both enhanced parallel to the direction of orientation. The technique presented here is simple and versatile in that it can be adapted for use with nanotubes synthesized by any method. In addition, the size of the BP can easily be increased using cylinders with larger dimensions. As a result, this approach offers an attractive route for producing large quantities of oriented BP at relatively low cost.

2. Experimental details

2.1. Materials

NC7000 MWCNTs with an average diameter of 10 nm and purity of 90% were supplied by Nanocyl, S.A. (Belgium). A surfactant, Triton X-100, was purchased from Fisher Scientific (Waltham, MA, USA). Nanotube dispersions were prepared by sonicating a mixture of 1.5 g MWCNTs, 15 mL surfactant, and 750 mL DI water with a horn (Fisher, sonic dismembrator model 100) for 2 h. The resulting dispersion was allowed to settle for 24 h, and the well-dispersed supernatant was used to prepare BP films with a setup shown schematically in **Fig. 1**.

Fig 1: Schematic of modified Taylor–Couette system used to simultaneously shear and filter MWCNT dispersions. (A colour version of this figure can be viewed online.)

2.2. Methods

The modified Taylor–Couette apparatus was constructed from an acrylic outer cylinder with an inner diameter of 31.15 mm and a high-density polyethylene Porex (Fairburn, GA, USA) inner cylinder having an outer diameter of 26.00 mm and an average porosity of 60 μm. The inner cylinder was sealed with adhesive tape along its length, except over an 8 cm long section. An electric stirring motor (Caframo, Ontario, Canada) with rpm control of ±1 rpm was used to rotate the outer cylinder at speeds up to 2000 rpm. Compression fitted PTFE bushings secured to the inner cylinder maintained the inner rod parallel to the outer cylinder while allowing the two to be separated easily. A small fill tube was inserted into a slit milled in the top bushing to provide fresh dispersion during filtration, and a vacuum in the inner cylinder was created by a belt-driven pump (Welch, Niles, IL, USA). In all experiments, the top of the inner cylinder was clamped to prevent rotation.

To fabricate BP using the setup, a 9 cm × 8 cm strip of nitrocellulose filter paper (Osmonics, Inc.) with an average pore size of 45 μm was affixed to the exposed porous section of the inner rod by pulling the paper tautly around the cylinder and bonding the overlapping ends of the paper with a small amount of adhesive. After the adhesive had cured, the inner cylinder was inserted into the outer cylinder and the gap was filled with dispersion. The outer cylinder was rotated at a constant rate to shear the fluid, and vacuum was subsequently applied to the fixed inner cylinder to force the dispersion through the filter paper. A BP sheet formed on the filter, and the separated water was collected in a series of traps. Fresh dispersion was continually added via the fill tube during filtration to maintain a constant fluid level.

After filtration, the inner cylinder was removed from the setup and the filter paper was cut along the overlapped edge to produce a rectangular sheet, which was dried in a vacuum oven at 100 °C for 12 h. The dried BP was then separated from the filter paper by gently folding and peeling the nanotube mat free from the filter. The resulting freestanding film of MWCNTs was soaked in isopropanol overnight in an attempt to remove residual surfactant before drying once more in a vacuum oven at 80 °C for 4 h. **Fig. 2** shows a representative sample of BP after processing. Despite washing with isopropanol, the final films likely contain some residual surfactant, as similar attempts to wash BP with alcohol have resulted in substantial but incomplete surfactant removal **[26]**, **[27]** and **[28]**.

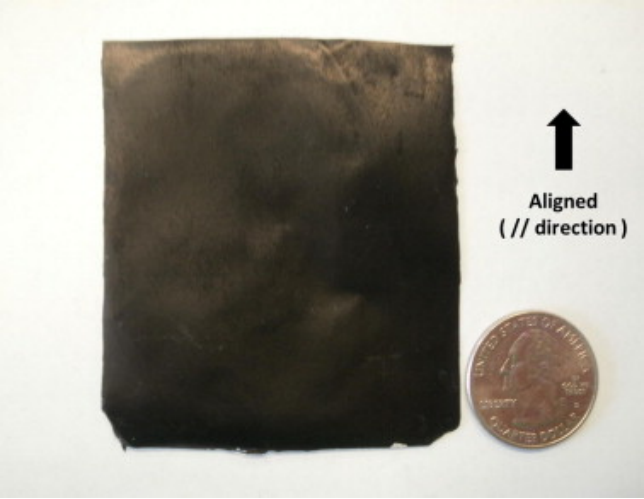

Fig 2: Optical image of dried BP sheet formed under a shear rate of 1000 s^{-1}.

2.3. Characterization

The viscosity of the MWCNT dispersions was measured as a function of shear rate using an AR2000ex rheometer equipped with a Peltier temperature control stage and a 40 mm diameter cone (α = 1°,0′,11″). Measurements were performed by placing 0.2 mL of dispersion on the Peltier stage and equilibrating at 25 °C before performing a constant temperature, steady-state flow test at shear rates ranging from 1 to 1200 s^{-1}. The degree of nanotube alignment in BP samples was monitored with scanning electron microscopy (SEM, FEI Quanta 200) operating at 8 kV accelerating voltage. Electrical conductivity measurements were performed using a linear four point probe (Jandel model RM2). For each test, a 1 cm × 3 cm strip was cut from the BP either perpendicular or parallel to the direction of alignment, and conductivity measurements were made to the top surface of the paper with the four probes oriented parallel to the long axis of the strip. The thickness of each sample was averaged from 10 measurements taken along the length of the BP using a digital micrometer (Mitutoyo). The anisotropic mechanical properties of BP samples was evaluated by tensile testing 0.5 cm × 3 cm × 100 μm strips cut either parallel or perpendicular to the direction of alignment. For each test, the BP strip was mounted in a flat-faced fixture and elongated with an Instron universal testing machine following a procedure similar to ASTM D882.

3. Results and discussion

3.1. Rheological behavior of the MWCNT dispersion

Fig. 3 depicts the rheological behavior of the MWCNT dispersion used in this study. In a similar manner to previous reports on aqueous nanotube dispersions **[29]** and **[30]**, the viscosity was observed to decrease significantly with increasing shear rate. This shear-thinning behavior is due to the fact that MWCNTs align under shear, which lowers their resistance to flow. The viscosity of the dispersion used in this study plateaus at ~800 s^{-1}, indicating that the nanotubes reach their maximum degree of alignment at shear rates above this value.

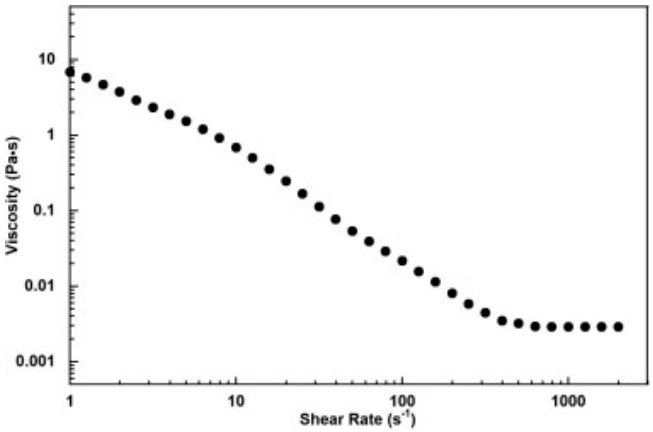

Fig 3: Rheological behavior of the aqueous MWCNT dispersion used in this study. (A colour version of this figure can be viewed online.)

3.2. Fabrication of aligned BP

The Taylor–Couette setup is a classic method for studying fluid behavior under shear. By rotating the outer and/or inner cylinder, shear forces develop in the fluid trapped between the two cylinders, the magnitude of which is determined by both their radii and relative speeds **[31]**. Rotation of the outer cylinder is desirable for aligning fibers in solution as it avoids turbulent transitions that can occur from instabilities associated with rotation of the inner cylinder **[32]**. The modified Taylor–Couette setup used in this study was designed to produce shear rates from 0 s^{-1} to 1200 s^{-1}. By shearing the dispersion while simultaneously applying a vacuum to the inner cylinder, the suspended nanotubes were circumferentially aligned and then forced onto filter paper. Progressive build-up of MWCNT layers led to the formation of BP comprised of nanotubes with a preferential orientation parallel to the circumference of the cylinders. In this paper, the direction of flow is referred to as "//", and the direction perpendicular to flow (the axial cylinder direction) is referred to as "⊥". The morphology of samples produced at various shear rates is depicted in **Fig. 4**, in which all of the micrographs were collected from the front side of the BP (side adjacent to cylinder gap). With no cylinder rotation (0 s^{-1}), the nanotubes are randomly oriented. As the shear rate is increased to 640 s^{-1}, the nanotubes become partially oriented in the // direction. At an even higher shear rate of 825 s^{-1}, the MWCNTs are highly aligned in the direction of flow. Shear rates above 825 s^{-1} also produced BP with MWCNTs oriented in the // direction, although a higher degree alignment is not discernible. Notably, the degree of alignment appears to vary somewhat through the thickness of the BP film. **Fig. S1** shows representative micrographs of BP produced at different shear rates as viewed form the backside of the films (side adjacent to filter paper). The degree of nanotube alignment seems diminished compared to the front side, possibly due to interactions among the nanotubes and filter paper fibers.

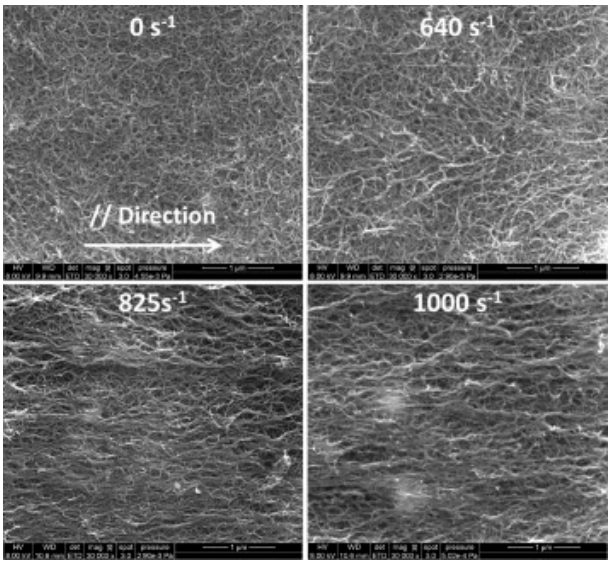

Fig 4: Scanning electron micrographs of BP formed at shear rates of 0 s^{-1}, 640 s^{-1}, 825 s^{-1}, and 1000 s^{-1}.

3.3. Electrical conductivity of BP

While SEM indicates alignment of MWCNTs in BP produced at elevated shear rates, it is a qualitative measure. To better quantify the degree of anisotropy, the electrical conductivity of BP samples was measured in different directions. **Fig. 5** contains representative current–voltage curves obtained from four point probe measurements of ~100 μm thick BP produced at shear rates of 0 s^{-1} and 1000 s^{-1}. BP formed at all shear rates displays ohmic behavior. However, random BP fabricated in the absence of shear exhibits very little directional dependence, while BP formed at a shear rate of 1000 s^{-1} has markedly lower slope (V/I) in the // direction and higher slope when measured ⊥ to alignment as a result of higher and lower conductivity, respectively. **Fig. 6** summarizes the electrical behavior of BP produced in this study as a function of shear rate and measurement direction. At low shear rates, the electrical anisotropy, defined as the ratio of conductivity measured // and ⊥ to alignment, is ~1. With increasing shear rate, the conductivity steadily increases // to alignment while decreasing in the ⊥ direction, and the anisotropy ratio reaches a plateau of ~2 around 825 s^{-1}. This behavior coincides with a plateau in shear thinning observed by rheology, and suggests that viscosity measurements are a convenient method for determining the minimum shear rate needed to maximize nanotube alignment.

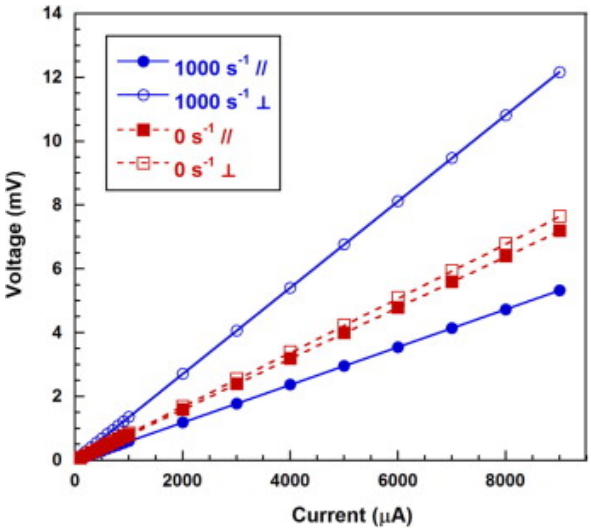

Fig 5: Representative I–V curves for BP samples produced in the absence of shear (red) and at $\dot{\gamma} = 1000\ s^{-1}$γ̇=1000s-1 (blue) measured both parallel and perpendicular to the direction of flow. (A colour version of this figure can be viewed online.)

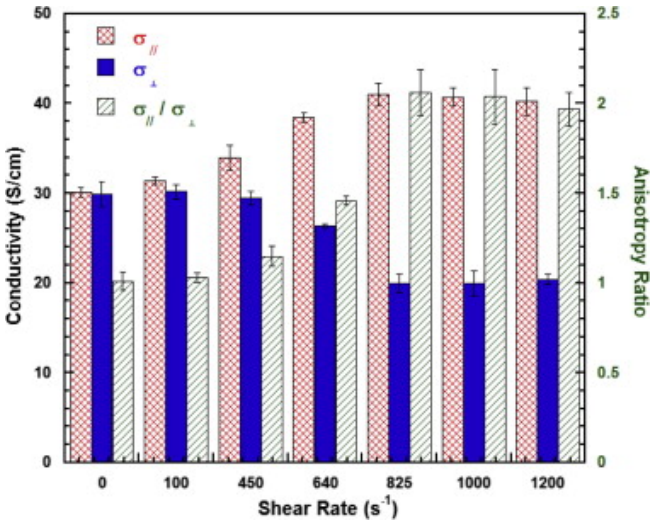

Fig 6: Summary of electrical conductivity measurements performed on BP in directions parallel and perpendicular to the direction of flow at various shear rates. (A colour version of this figure can be viewed online.)

Conductivity in BP is generally dictated by nanotube-nanotube junctions, which limit the mean free paths of electrons and lower the conductivity **[33]** and **[34]**. The BP produced in this study does not contain perfectly aligned MWCNTs, and as a result, nanotube-nanotube junctions play a role in the conductivity in all directions. However, electrons traveling in the // direction of aligned BP samples will encounter far fewer junctions than electrons traveling in the transverse direction, and, as a result will experience less resistance. Anisotropic electrical conductivity has been observed in aligned BP samples produced by other methods, and **Table 1** compares the results of this study with a select number of those previously reported in the literature. Here we

report a maximum anisotropy of ~2, which is lower than that achieved using magnetic alignment and pulling of VACNTs, but similar to the value found by "domino pushing" MWCNT forests.

Table 1.

Literature reports of electrical anisotropy in aligned BP at room temperature.

Method	$\sigma_{//}$ (S/cm)	$\sigma_{\perp}$ (S/cm)	$\sigma_{//}/\sigma_{\perp}$	Reference
Magnetic alignment				
SWCNT	1100	138	8.0	[37]
SWCNT	1210	200	6.1	[38]
Pushing/pulling VACNT				
MWCNT	209	110	1.9	[39]
MWCNT	403	56	7.2	[34]
Mechanical stretching				
Nanomp MWCNT[a]	600	–	–	[5]

[a] Study did not report $\sigma_{\perp}$ but did find that $\sigma_{//}$ was 40% higher than randomly oriented BP.

The lower levels of anisotropy found in this study may be due to the presence of a higher number of misaligned nanotubes than by magnetic alignment. Because the relaxation time of water is very short, the aqueous dispersions used in this study may have allowed some MWCNTs to relax and coil upon removal of shear forces, especially on the upper few layers, which are less constrained by neighboring nanotubes. The use of higher viscosity fluids may limit such relaxation and improve nanotube alignment and packing density. Previous studies of CNT alignment in polymer composites have shown that shearing CNTs in a viscous resin can produce high degrees of stable alignment and subsequently large increases in conductivity in the aligned direction **[35]** and **[36]**. Greater levels of alignment might also be achieved by tuning the interaction among the nanotubes, surfactant, and filter paper, and greater mechanical and electrical properties could be realized by extending the approach to other varieties of CNTs such as high aspect ratio SWCNTs.

3.4. Mechanical properties of BP

The anisotropic mechanical properties of random BP produced in the absence of shear and at a shear rate of 1000 s^{-1} were also investigated to test the efficacy of BP for composite applications. Fig. 7 shows representative stress–strain curves for BP tested at both shear rates in different directions. The results of testing many samples are summarized in Fig. 8. Randomly oriented BP has a modulus of ~0.4 GP, ultimate tensile strength near 4 MPa, and a strain at break of 1% with no directional dependence within experimental error. In contrast, BP produced under high shear shows strong anisotropy, with moduli and tensile strengths 2.8 and 2.2 times higher in the direction of alignment, respectively. However, even in the direction of alignment, the mechanical properties are modest, and further improvements are likely needed before the BP can be considered for use as reinforcement in composites.

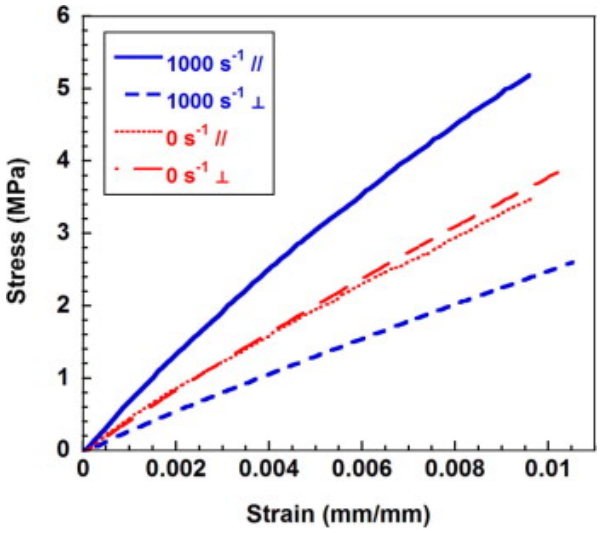

Fig 7: Representative stress–strain curves for BP produced in the absence of shear and at $\dot{\gamma} = 1000\ s^{-1}$ γ̇=1000s-1 in directions both parallel and perpendicular to flow. (A colour version of this figure can be viewed online.)

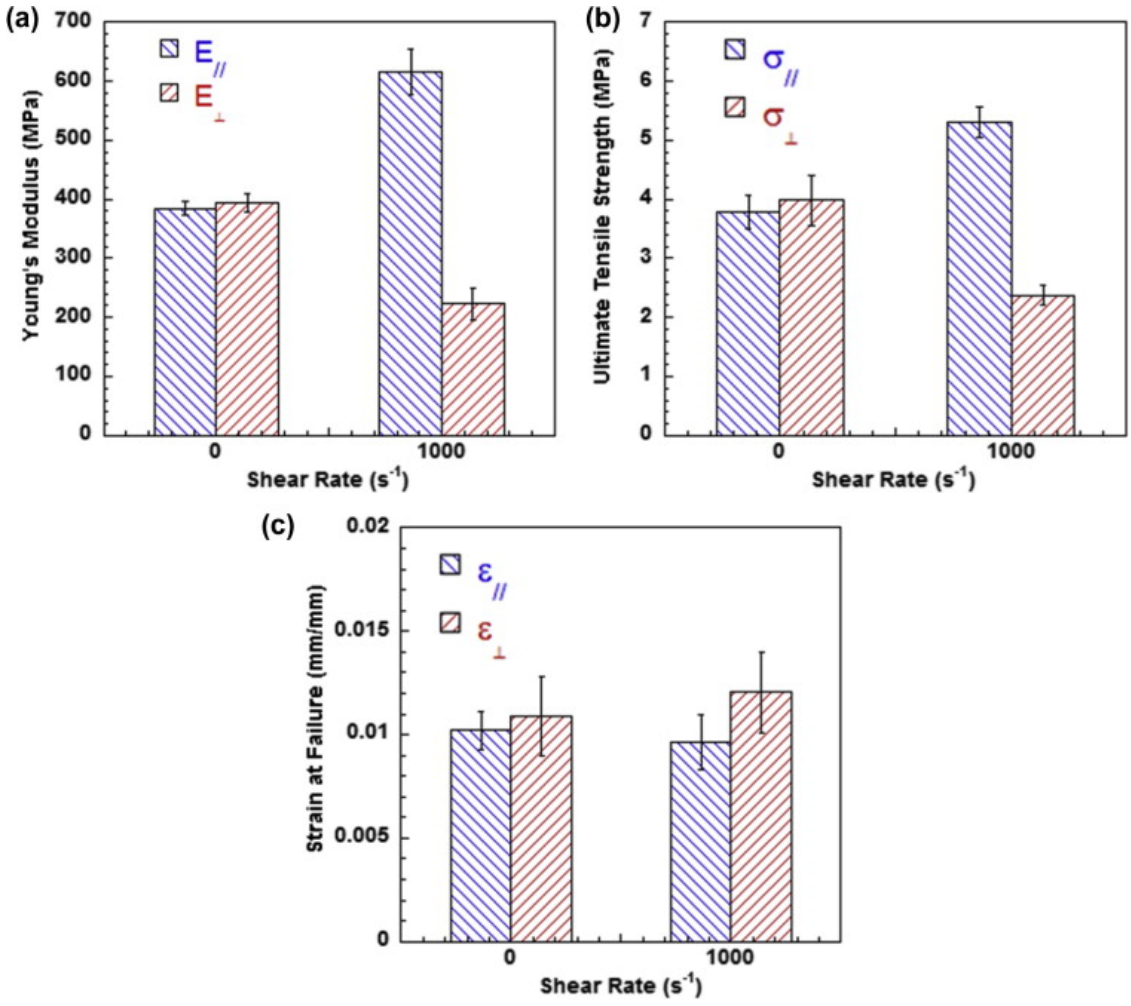

Fig 8: Summary of mechanical properties for BP prepared in the absence of shear and at $\dot{\gamma} = 1000\ s^{-1}$ γ̇=1000s-1 in directions both parallel (▧) and perpendicular to flow (▨). (A colour version of this figure can be viewed online.)

4. Conclusions

A simple method for aligning nanotubes in BP with a modified Taylor–Couette system has reported. Simultaneous shear-alignment and filtration of an aqueous MWCNT dispersion yielded BP with preferential nanotube orientation in the direction of flow. The BP exhibited anisotropic electrical and mechanical properties, which were both enhanced parallel to the direction of orientation and maximized at high shear rates. While the highest degree of anisotropy was found to be lower than some previously reported methods, such as magnetic alignment, the technique presented here is simple and versatile in that it can be adapted for use with any type of CNT synthesized by any method. In addition, large BP sheets can be easily fabricated by increasing the length and diameter of the cylinders in the setup, making this approach an attractive route for the producing large quantities of oriented BP at relatively low cost.

Appendix A. Supplementary data

See supplementary document.

Scanning electron micrographs of the backside of BP formed at shear rates of 0 s^{-1}, 640 s^{-1}, 825 s^{-1}, and 1000 s^{-1}.

References

1. M. Moniruzzaman, K.I. Winey. Polymer nanocomposites containing carbon nanotubes. Macromolecules, 39 (16) (2006), pp. 5194–5205

2. B. Fiedler, F.H. Gojny, M.H.G. Wichmann, M.C.M. Nolte, K. Schulte. Fundamental aspects of nano-reinforced composites. Compo Sci Technol, 66 (16) (2006), pp. 3115–3125

3. Z. Wang, Z. Liang, B. Wang, C. Zhang, L. Kramer. Processing and property investigation of single-walled carbon nanotube (SWNT) buckypaper/epoxy resin matrix nanocomposites. Compos Part A: Appl Sci Manuf, 35 (10) (2004), pp. 1225–1232

4. B. Ashrafi, J. Guan, V. Mirjalili, P. Hubert, B. Simard, A. Johnston. Correlation between young's modulus and impregnation quality of epoxy-impregnated SWCNT buckypaper. Compos Part A: Appl Sci Manuf, 41 (9) (2010), pp. 1184–1191

5. Q. Cheng, J. Bao, J. Park, Z. Liang, C. Zhang, B. Wang. High mechanical performance composite conductor: multi-walled carbon nanotube sheet/bismaleimide nanocomposites. Adv Funct Mater, 19 (20) (2009), pp. 3219–3225

6. T.P. Giang, P. Young-Bin, W. Shiren, L. Zhiyong, W. Ben, Z. Chuck, *et al.* Mechanical and electrical properties of polycarbonate nanotube buckypaper composite sheets. Nanotechnology, 19 (32) (2008), p. 325705

7. H. Guo, T.V. Sreekumar, T. Liu, M. Minus, S. Kumar. Structure and properties of polyacrylonitrile/single wall carbon nanotube composite films. Polymer, 46 (9) (2005), pp. 3001–3005

8. P. Gonnet, Z. Liang, E.S. Choi, R.S. Kadambala, C. Zhang, J.S. Brooks, *et al.* Thermal conductivity of magnetically aligned carbon nanotube buckypapers and nanocomposites. Curr Appl Phys, 6 (1) (2006), pp. 119–122

9. P. Jin Gyu, L. Jeffrey, C. Qunfeng, B. Jianwen, S. Jesse, L. Richard, *et al.* Electromagnetic interference shielding properties of carbon nanotube buckypaper composites. Nanotechnology, 20 (41) (2009), p. 415702

10. Q. Cheng, B. Wang, C. Zhang, Z. Liang. Functionalized carbon-nanotube sheet/bismaleimide nanocomposites: mechanical and electrical performance beyond carbon–fiber composites. Small, 6 (6) (2010), pp. 763–767

11. K. Jiang, Q. Li, S. Fan. Nanotechnology: spinning continuous carbon nanotube yarns. Nature, 419 (6909) (2002), p. 801

12. M. Zhang, S. Fang, A.A. Zakhidov, S.B. Lee, A.E. Aliev, C.D. Williams, *et al.* Strong, transparent, multifunctional, carbon nanotube sheets. Science, 309 (5738) (2005), pp. 1215–1219

13. X. Zhang, Q. Li, T.G. Holesinger, P.N. Arendt, J. Huang, P.D. Kirven, *et al.* Ultrastrong, stiff, and lightweight carbon-nanotube fibers. Adv Mater, 19 (23) (2007), pp. 4198–4201

14. M. Zhang, K.R. Atkinson, R.H. Baughman. Multifunctional carbon nanotube yarns by downsizing an ancient technology. Science, 306 (5700) (2004), pp. 1358–1361

15. K. Liu, Y. Sun, X. Lin, R. Zhou, J. Wang, S. Fan, *et al.* Scratch-resistant, highly conductive, and high-strength carbon nanotube-based composite yarns. ACS Nano, 4 (10) (2010), pp. 5827–5834

16. K. Liu, Y. Sun, R. Zhou, H. Zhu, J. Wang, L. Liu, *et al.* Carbon nanotube yarns with high tensile strength made by a twisting and shrinking method. Nanotechnology, 21 (4) (2010), p. 045708

17. M.D. Lima, S. Fang, X. Lepró, C. Lewis, R. Ovalle-Robles, J. Carretero-González, *et al.* Biscrolling nanotube sheets and functional guests into yarns. Science, 331 (6013) (2011), pp. 51–55

18. W. Li, C. Jayasinghe, V. Shanov, M. Schulz. Spinning carbon nanotube nanothread under a scanning electron microscope. Materials, 4 (9) (2011), pp. 1519–1527

19. W. Liu, X. Zhang, G. Xu, P.D. Bradford, X. Wang, H. Zhao, *et al.* Producing superior composites by winding carbon nanotubes onto a mandrel under a poly (vinyl alcohol) spray. Carbon, 49 (14) (2011), pp. 4786–4791

20. W. Ding, S. Pengcheng, L. Changhong, W. Wei, F. Shoushan. Highly oriented carbon nanotube papers made of aligned carbon nanotubes. Nanotechnology, 19 (7) (2008), p. 075609

21. D.A. Walters, M.J. Casavant, X.C. Qin, C.B. Huffman, P.J. Boul, L.M. Ericson, *et al.* In-plane-aligned membranes of carbon nanotubes. Chem Phys Lett, 338 (1) (2001), pp. 14–20

22. J.G. Park, J. Smithyman, C.-Y. Lin, A. Cooke, A.W. Kismarahardja, S. Li, *et al.* Effects of surfactants and alignment on the physical properties of single-walled carbon nanotube buckypaper. J Appl Phys, 106 (10) (2009), pp. 104310–104316

23. J.P. Lu. Novel magnetic properties of carbon nanotubes. Phys Rev Lett, 74 (7) (1995), pp. 1123–1126

24. L. Wang, P.S. Davids, A. Saxena, A.R. Bishop. Correlation effects and electronic properties of fullerenes and carbon nanotubes. J Phys Chem Solids, 54 (11) (1993), pp. 1493–1496

25. M.F. Lin, K.W.K. Shung. Magnetization of graphene tubules. Phys Rev B, 52 (11) (1995), pp. 8423–8438

26. Q. Wu, W. Zhu, C. Zhang, Z. Liang, B. Wang. Study of fire retardant behavior of carbon nanotube membranes and carbon nanofiber paper in carbon fiber reinforced epoxy composites. Carbon, 48 (6) (2010), pp. 1799–1806

27. I.-W.P. Chen, R. Liang, H. Zhao, B. Wang, C. Zhang. Highly conductive carbon nanotube buckypapers with improved doping stability via conjugational cross-linking. Nanotechnology, 22 (48) (2011), p. 485708

28. Lin C-Y. Investigation and characterization of SWNT buckypaper manufacturing process [MS thesis]. Tallahassee, FL, USA: Florida State University; 2005.

29. Y. Ding, H. Alias, D. Wen, R.A. Williams. Heat transfer of aqueous suspensions of carbon nanotubes (CNT nanofluids). Int J Heat and Mass Transfer, 49 (1–2) (2006), pp. 240–250

30. S. Halelfadl, P. Estellé, B. Aladag, N. Doner, T. Maré. Viscosity of carbon nanotubes water-based nanofluids: influence of concentration and temperature. Int J Therm Sci, 71 (2013), pp. 111–117

31. R. Darby. Chemical engineering fluid mechanics. Marcel Dekker, New York (2001)

32. C.D. Andereck, S.S. Liu, H.L. Swinney. Flow regimes in a circular Couette system with independently rotating cylinders. J Fluid Mech, 164 (1986), pp. 155–183

33. D.J. Yang, S.G. Wang, Q. Zhang, P.J. Sellin, G. Chen. Thermal and electrical transport in multi-walled carbon nanotubes. Phys Lett A, 329 (3) (2004), pp. 207–213

34. Y. Inoue, Y. Suzuki, Y. Minami, J. Muramatsu, Y. Shimamura, K. Suzuki, *et al.* Anisotropic carbon nanotube papers fabricated from multiwalled carbon nanotube webs. Carbon, 49 (7) (2011), pp. 2437–2443

35. L.J. Lanticse, Y. Tanabe, K. Matsui, Y. Kaburagi, K. Suda, M. Hoteida, *et al.* Shear-induced preferential alignment of carbon nanotubes resulted in anisotropic electrical conductivity of polymer composites. Carbon, 44 (14) (2006), pp. 3078–3086

36. F. Du, J.E. Fischer, K.I. Winey. Effect of nanotube alignment on percolation conductivity in carbon nanotube/polymer composites. Phys Rev B, 72 (12) (2005), p. 121404

37. J.E. Fischer, W. Zhou, J. Vavro, M.C. Llaguno, C. Guthy, R. Haggenmueller, *et al.* Magnetically aligned single wall carbon nanotube films: preferred orientation and anisotropic transport properties. J Appl Phys, 93 (4) (2003), pp. 2157–2163

38. J. Hone, M.C. Llaguno, N.M. Nemes, A.T. Johnson, J.E. Fischer, D.A. Walters, *et al.* Electrical and thermal transport properties of magnetically aligned single wall carbon nanotube films. Appl Phys Lett, 77 (5) (2000), pp. 666–668

39. D. Wang, P. Song, C. Liu, W. Wu, S. Fan. Highly oriented carbon nanotube papers made of aligned carbon nanotubes. Nanotechnology, 19 (7) (2008), p. 075609